

Critical exponents for the FPL² model

David Dei Cont and Bernard Nienhuis

*Instituut voor Theoretische Fysica, Universiteit van Amsterdam,
Valckenierstraat 65, 1018 XE Amsterdam, The Netherlands*
deicont@science.uva.nl, nienhuis@science.uva.nl

Abstract

Starting from the Bethe ansatz solution we derive a set of coupled non-linear integral equations for the fully packed double loop model (FPL²) on the square lattice. As an application we find exact expressions for the central charge and for the scaling dimension corresponding to the simplest charge excitation. We study numerically the low-lying excitations corresponding to more general perturbations of the ground state and discover that the corresponding scaling dimensions are well described by the Cartan matrix of sl_4 .

Key words: loops, Bethe ansatz, non-linear integral equation, central charge, scaling dimensions.

1 Introduction

The fully packed double loop model (FPL²) is a two dimensional statistical model constructed by decorating the square lattice with two species of loops (black and grey), under the constraint that every lattice edge is covered by only one loop and every vertex is visited by both types of loops.

It exhibits a rich phase diagram and provides a representation for previously studied models: Ice model [15], four-colouring model [14, 11, 12, 2], dimer loop model [29], double Hamiltonian walk [10] and compact polymers [28]. A generalization of the FPL² model, which offers a unifying picture of the compact, dense and dilute phase of polymers, was proposed in [8] by relaxing the full packing constraint. Another possible generalization corresponds to the Flory model of polymer melting [6, 7].

Jacobsen and Kondev mapped the FPL² model onto a height model and postulate that the long wavelength behaviour is correctly described by a Liouville field theory. Making use of the Coulomb gas method they succeed in computing the central charge and the critical exponents [4, 9]. The study of the relation between the Coulomb gas representation and the underlying conformal field theory has been initiated in [21].

Recently we mapped the FPL² model onto a 24-vertex model and diagonalized the corresponding transfer matrix by means of coordinate Bethe ansatz (BA) [1, 2]. The solution holds only when the two loop fugacities are the same. In particular we calculated analytically the configurational entropy for the double Hamiltonian walk and the four-coloring model. We also confirmed a conjecture on the average length of loops [5]. In the particular limit in which the fugacities of the loops are both equal to two, the BA equations become rational [2] and look very much like those derived in [25] for mixed SU(N) vertex model for the case $N = 4$.

When we made this paper ready for publication, Jacobsen and Zinn-Justin [3] succeed in finding a Yang-Baxter structure, for the FPL² model, in terms of the affine quantum group $U_q(\widehat{sl(4)})$. They reobtain the BA equations following the algebraic approach and write exact expressions for the central charge and for the scaling dimensions of the low-lying excitations.

These quantities can be calculated from the leading finite-size corrections to the ground [18, 19] and the excited [16, 17] energies. Analytical calculations, for the low-lying excitations of models solvable by the Bethe ansatz equations, were done in [22, 23]. An analytical method, based on the construction of a non-linear integral equation (NLIE) for the counting function, which allows the calculation of the central charge, has been developed in [33, 32]. This method has been exploited in [33, 30, 31, 35, 36, 37] in order to include excitations. The case of multicomponent BA equations has been investigated in [34].

Here, following [34], we write a non-linear integral equation for the FPL² model in the presence of the seam. As an application we compute analytically the value of the central charge and of the scaling dimension corresponding to one grey and one black string prop-

agating between two points of the lattice. Our results are in agreement with the results found in [4] via the field theory. We also studied numerically the low-lying excitations [26] generated by varying the number of particles (charge excitations), allowing transitions from one side to the other of the Fermi seas (umklapp processes) and perturbing the surfaces of the Fermi seas (particle-hole excitations) [22]. It turns out that the scaling dimensions are well described by a compact formula [23] through the Cartan matrix of sl_4 . Our results coincide with those found in [3].

The present work is organized as follows. In section 2 we introduce the FPL^2 model, summarize the main results of [1] and define the counting functions. For completeness in section 3 we show in detail how the finite sums entering in the definition of the counting functions can be expressed in terms of integrals involving the counting functions. This procedure is well known in the literature. See for instance [31, 34]. In section 4 we derive a set of coupled non-linear integral equations for the counting functions, in the presence of the seam. An integral expression for the finite-size free energy is derived in section 5. The central charge is calculated in section 6 and the scaling dimension associated with one grey and one black string derived in section 7. In section 8 we study numerically the low-lying excitations.

2 The model

The fully packed double loop model (FPL^2) is a two dimensional statistical model constructed decorating the square lattice with two species of loops. Each bond of the square lattice is covered by only one loop and every vertex is visited by both types of loops. Loops of the same type are not allowed to cross. Representing the two species by black and grey segments respectively, the fully-packing constraint forces each vertex of the square lattice to have one of the six appearances depicted in figure 1. We place the model on a cylinder of circumference L and height M with periodic boundary conditions also in the vertical



Figure 1: The six vertex configurations of the FPL^2 model that are allowed by the fully-packing constraint. Each vertex is visited by both types of loops. The two rightmost vertices permit the two species to cross. If we assign an orientation to the loops we obtain 24 distinct vertices.

direction. The partition function is defined by:

$$Z(L, M) = \sum n_b^{N_b} n_g^{N_g} m_b^{M_b} m_g^{M_g} \quad (1)$$

where the sum runs over all the allowed configurations. The exponents N_b and N_g are the respective numbers of black and grey contractable loops. Since the model is placed on a cylinder loops are allowed to wind. We denote by M_b and M_g the number of black and grey winding loops. We assign the fugacities $n_{b,g}$ for contractable loops and $m_{b,g}$ for uncontractable ones.

In [1] we map the loop model into a 24-vertex model and construct the transfer matrix \mathbf{T} . The partition function is the sum of the eigenvalues Λ_i of the transfer matrix, raised to the power M :

$$Z(L, M) = \text{Tr } \mathbf{T}^M(L) = \sum \Lambda_i^M(L). \quad (2)$$

In the limit in which the height of the cylinder extend to infinite $M \rightarrow \infty$ the finite-size free energy density $f(L)$ can be expressed in terms of the largest eigenvalue $\Lambda_0(L)$ of the transfer matrix:

$$f(L) = -\frac{1}{L} \log \Lambda_0(L). \quad (3)$$

At criticality, the dominant finite-size correction of the free energy density, can be related to the central charge c and the bulk free energy $f(\infty)$ via the formula [18, 19]:

$$f(L) = f(\infty) - \frac{c \pi}{6 L^2} + o(1/L^2). \quad (4)$$

The subdominant eigenvalues Λ_i allow the computation of the scaling dimensions Δ_i thanks to the formula [16, 17]:

$$\log \frac{\Lambda_0(L)}{\Lambda_i(L)} = \frac{2 \pi}{L} \Delta_i + o(1/L). \quad (5)$$

In [1] we show that the model is solvable in the particular case in which the fugacities are the same ($n_b = n_g$ and $m_b = m_g$). The transfer matrix is diagonalized using coordinate nested Bethe ansatz and an analytical expression for the free energy, in the thermodynamic limit, is derived. In particular we find the free energy of the four-coloring model [11, 12, 2] and the double Hamiltonian walk [10] and recover the known entropy of the Ice model [15]. Let us summarize the main result of [1]: The fugacities entering in the partition sum (1) are expressed in terms of two phases θ and α , through the relations:

$$n_b = n_g = 2 \cos \pi \theta \quad m_b = m_g = 2 \cos \pi \alpha \quad 0 \leq \theta, \alpha \leq 1 \quad (6)$$

and a θ -dependent function is introduced:

$$S_c(x, \theta) \equiv \frac{\sin \frac{\pi \theta}{2}(c + x i)}{\sin \frac{\pi \theta}{2}(c - x i)}. \quad (7)$$

With these definitions the Bethe ansatz equations (BAE) assume the form:

$$S_1(u_j, \theta)^{L/2} = - \prod_{i=1}^{n_w} S_1(w_i - u_j, \theta) \prod_{k=1}^{n_u} -S_2(u_j - u_k, \theta) \quad (8)$$

$$S_1(v_j, \theta)^{L/2} = - \prod_{i=1}^{n_w} S_1(w_i - v_j, \theta) \prod_{k=1}^{n_v} -S_2(v_j - v_k, \theta) \quad (9)$$

$$\exp(-2i\pi\alpha) \prod_{j=1}^{n_u} S_1(w_l - u_j, \theta) \prod_{k=1}^{n_v} S_1(w_l - v_k, \theta) \prod_{m=1}^{n_w} -S_2(w_m - w_l, \theta) = -1. \quad (10)$$

Every solution of the previous equations, with non coinciding roots, is in correspondence with an eigenvalue of the transfer matrix via the expression:

$$\Lambda = (-1)^{n_w} \left[\exp(i\pi\alpha) \prod_{j=1}^{n_u} S_1(u_j, \theta)^{1/2} \prod_{k=1}^{n_v} S_1(v_k, \theta)^{1/2} \prod_{m=1}^{n_w} \frac{\sin \frac{\pi\theta}{2}(w_m i - 2)}{\sin \frac{\pi\theta}{2} w_m i} \right. \\ \left. + \exp(-i\pi\alpha) \prod_{j=1}^{n_u} S_1(u_j, \theta)^{-1/2} \prod_{k=1}^{n_v} S_1(v_k, \theta)^{-1/2} \prod_{m=1}^{n_w} \frac{\sin \frac{\pi\theta}{2}(w_m i + 2)}{\sin \frac{\pi\theta}{2} w_m i} \right]. \quad (11)$$

In [4] the central charge and a set of scaling dimensions were computed analytically but not rigorously via the field theory making use of Coulomb gas techniques. In this paper we are going to compute the conformal quantities starting from the Bethe ansatz solution. These results are included in the independent and recent paper [3].

The calculation is based on the formula (4) and (5) that relate the central charge and the scaling dimensions to the leading finite-size correction of the ground and excited energies. An analytical method, based on the perturbation of the Fermi sea, was developed for the first time in [22, 23]. Later another method, based on the construction of a non-linear integral equation, was developed. Following this method the central charge, of models solvable by Bethe ansatz equations, was calculated in [33, 32] and the scaling dimensions in [33, 35, 36, 37]. The method has been refined to include string excitations [31] and multicomponents BA equations [34]. Here we are going to follow this last approach. The central objects which enter in this machinery are the counting functions $Z_{L,s}$ defined by:

$$Z_{L,u}(u, \theta) \equiv -\frac{L}{2} \phi_1(u, \theta) + \sum_{m=1}^{n_w} \phi_1(w_m - u, \theta) - \sum_{k=1}^{n_u} \phi_2(u_k - u, \theta) \\ Z_{L,w}(w, \theta) \equiv \sum_{j=1}^{n_u} \phi_1(u_j - w, \theta) + \sum_{k=1}^{n_v} \phi_1(v_k - w, \theta) - \sum_{l=1}^{n_w} \phi_2(w_l - w, \theta) - 2\pi\alpha \quad (12) \\ Z_{L,v}(v, \theta) \equiv -\frac{L}{2} \phi_1(v, \theta) + \sum_{m=1}^{n_w} \phi_1(w_m - v, \theta) - \sum_{k=1}^{n_v} \phi_2(v_k - v, \theta)$$

where the following function has been defined:

$$\phi_c(x, \theta) \equiv i \log S_c(x, \theta). \quad (13)$$

Notice that the counting functions are constructed by taking the logarithm of the equations (8-10). The key property of $Z_{L,s}$ is that it counts the BA roots, in the sense that for each root $\lambda_{s,k}$ of the BAE (8-10) we have:

$$Z_{L,s}(\lambda_{s,k}) = 2\pi I_{s,k} \quad k = 1, \dots, n_s \quad s = u, w, v \quad (14)$$

where $I_{s,k}$ is an integer or half-integer number, depending on the number of roots of each type. We will call holes, objects $h_{s,k}$ that are counted by $Z_{L,s}$:

$$Z_{L,s}(h_{s,k}) = 2\pi I_{H,s,k} \quad k = 1, \dots, n_s \quad s = u, w, v \quad (15)$$

but are not solution of the system of BA equations (8-10). Where $I_{H,s,k}$ are integers or half-integer numbers. The first step towards the exact calculation of the finite-size corrections consists in the replacement of the *finite* sums in the rhs of (12) by integrals. In the next section we are going to show how this is possible.

3 From a finite sum to an integral

We want to find an integral expression for the finite sums entering in the counting functions (12) for the particular case in which the BA roots $\lambda_{s,k}$ are positioned on the real line and no real holes are present. These sums have the general form:

$$\sum_{k=1}^{n_s} \phi_c(\lambda_{s,k} - \lambda, \theta). \quad (16)$$

Start by noting that with the help of the counting function it is possible to construct a function which is analytic in all the complex plane and has zeros of order one at the BA roots. In fact, the following expression satisfies the requirements:

$$1 + (-1)^\delta \exp[i Z_{L,s}(z)] \quad (17)$$

where we choose $\delta = 1$ for the case in which the number of roots is such that $Z_{L,s}(\lambda_{s,k})/\pi$ is even and $\delta = 0$ when it is odd. Applying Cauchy formula we can prove the identity:

$$2\pi i \sum_{k=1}^{n_s} \phi_c(\lambda_{s,k} - \lambda, \theta) = \int_{\Gamma} d\mu \phi_c(\mu - \lambda, \theta) \frac{i Z'_{L,s}(\mu) (-1)^\delta \exp[i Z_{L,s}(\mu)]}{1 + (-1)^\delta \exp[i Z_{L,s}(\mu)]} \quad (18)$$

where Γ is a close contour which encircles counterclockwise the BA roots $\lambda_{s,k}$. A fundamental assumption for the validity of the previous equality is the analyticity of $\phi_c(z, \theta)$ inside and on the contour Γ . In the following we will use the shorthand notation:

$$R_{s,\delta}(z) \equiv \frac{i Z'_{L,s}(z) (-1)^\delta \exp[i Z_{L,s}(z)]}{1 + (-1)^\delta \exp[i Z_{L,s}(z)]}. \quad (19)$$

We assumed that the roots of the BA equations were located on the real axis. Therefore we choose for Γ a box centered at the origin, extending from $-\infty$ to $+\infty$ in the horizontal direction and of height 2η , and integrate counterclockwise. In the limit $\eta \rightarrow 0^+$ only the integrals running on the side parallel to the real axis survive and the rhs of (18) becomes:

$$\int_{\Gamma} d\mu \phi_c(\mu - \lambda, \theta) R_{s,\delta}(\mu) = \lim_{\eta \rightarrow 0^+} \left[\int_{-\infty}^{+\infty} dx \phi_c(x - i\eta - \lambda, \theta) R_{s,\delta}(x - i\eta) \right. \\ \left. + \int_{+\infty}^{-\infty} dx \phi_c(x + i\eta - \lambda, \theta) R_{s,\delta}(x + i\eta) \right]. \quad (20)$$

The next step consists in the manipulation of the expressions $R_{s,\delta}(x + i\eta)$ and $R_{s,\delta}(x - i\eta)$. At a first glance one would say that:

$$R_{s,\delta}(x \pm i\eta) = \frac{d}{dx} \log \left[1 + (-1)^\delta \exp[iZ_{L,s}(x \pm i\eta)] \right]. \quad (21)$$

But this is not always true because the logarithm has a cut on the negative real line. We analyze this point in more details focusing on the term $R_{s,\delta}(x + i\eta)$. Let us study the behaviour of the argument of the logarithm in a neighborhood of a solution x of the BA equations. To construct the neighborhood take a small real number ϵ and remind that $\eta > 0$. The following expansion hold:

$$1 + (-1)^\delta \exp[iZ_{L,s}(x + \epsilon + i\eta)] = (\eta - i\epsilon) Z'_{L,s}(x) + \mathcal{O}((\epsilon + i\eta)^2). \quad (22)$$

From this expansion we see that if $Z'_{L,s}(x) > 0$ the argument of the logarithm has a positive real part. Thus varying ϵ it will never cross the cut and the equality (21) is satisfied. On the other hand if $y_{s,k}$ is a solution of the BAE for which $Z'_{L,s}(y_{s,k}) < 0$ (we call $y_{s,k}$ a special object) the logarithm will exhibit a discontinuity at $\epsilon = 0$. However the expression $R_{s,\delta}(x + i\eta)$ is continuous when x runs from $-\infty$ to $+\infty$ and so it must be the derivative of a continuous function. Thus in the presence of special objects $y_{s,k}$ relation (21) must be replaced with the following equality:

$$R_{s,\delta}(x + i\eta) = \frac{d}{dx} \log \left[1 + (-1)^\delta \exp[iZ_{L,s}(x + i\eta)] \right] + 2\pi i \sum_{k=1}^{n_{y_s}} \delta(x - y_{s,k}). \quad (23)$$

It can be proved that a similar relation holds for $R_{s,\delta}(x - i\eta)$:

$$R_{s,\delta}(x - i\eta) = i Z'_{L,s}(x - i\eta) + \frac{d}{dx} \log \left[1 + (-1)^\delta \exp[-iZ_{L,s}(x - i\eta)] \right] - 2\pi i \sum_{k=1}^{n_{y_s}} \delta(x - y_{s,k}). \quad (24)$$

Comparing this equality with (23) we see that the special objects contribute with the opposite sign and that the extra term $Z'(x - i\eta)$ arises. Substituting (23) and (24) into

(20) yields:

$$\begin{aligned}
\int_{\Gamma} d\mu \phi_c(\mu - \lambda, \theta) R_{s,\delta}(\mu) &= i \int_{-\infty}^{+\infty} dx \phi_c(x - i\eta - \lambda, \theta) Z'_{L,s}(x - i\eta) \\
&+ \int_{-\infty}^{+\infty} dx \phi_c(x - i\eta - \lambda, \theta) \frac{d}{dx} \log \left[1 + (-1)^\delta \exp[-iZ_{L,s}(x - i\eta)] \right] \\
&- \int_{-\infty}^{+\infty} dx \phi_c(x + i\eta - \lambda, \theta) \frac{d}{dx} \log \left[1 + (-1)^\delta \exp[iZ_{L,s}(x + i\eta)] \right] \\
&- 2\pi i \sum_{k=1}^{n_{y_s}} \phi_c(y_{s,k} - i\eta - \lambda, \theta) - 2\pi i \sum_{k=1}^{n_{y_s}} \phi_c(y_{s,k} + i\eta - \lambda, \theta).
\end{aligned} \tag{25}$$

From the definitions (7,13,12) we see that the functions $Z_{L,s}$ and ϕ_c enjoy the following symmetry (since α and θ are real numbers):

$$\phi_c(z, \theta) = \overline{\phi_c(\bar{z}, \theta)} = -\phi_c(-z, \theta) \quad Z_{L,s}(z) = \overline{Z_{L,s}(\bar{z})} \tag{26}$$

so that we can write the compact formula:

$$\begin{aligned}
\int_{\Gamma} d\mu \phi_c(\mu - \lambda, \theta) R_{s,\delta}(\mu) &= i \int_{-\infty}^{+\infty} dx \phi_c(x - i\eta - \lambda, \theta) Z'_{L,s}(x - i\eta) \\
&- 2i \operatorname{Im} \int_{-\infty}^{+\infty} dx \phi_c(x + i\eta - \lambda, \theta) \frac{d}{dx} \log \left[1 + (-1)^\delta \exp[iZ_{L,s}(x + i\eta)] \right]
\end{aligned} \tag{27}$$

where we dropped the terms containing the special objects because for the finite-size corrections that we will investigate they do not appear. Integrating by parts:

$$\begin{aligned}
\int_{\Gamma} d\mu \phi_c(\mu - \lambda, \theta) R_{s,\delta}(\mu) &= i \phi_c(x - i\eta - \lambda, \theta) Z_{L,s}(x - i\eta) \Big|_{x=-\infty}^{x=+\infty} \\
&- i \int_{-\infty}^{+\infty} dx \phi'_c(x - i\eta - \lambda, \theta) Z_{L,s}(x - i\eta) \\
&- 2i \operatorname{Im} \phi_c(x + i\eta - \lambda, \theta) \log \left[1 + (-1)^\delta \exp[iZ_{L,s}(x + i\eta)] \right] \Big|_{x=-\infty}^{x=+\infty} \\
&+ 2i \operatorname{Im} \int_{-\infty}^{+\infty} dx \phi'_c(x + i\eta - \lambda, \theta) \log \left[1 + (-1)^\delta \exp[iZ_{L,s}(x + i\eta)] \right].
\end{aligned} \tag{28}$$

The line of integration of the first integral can be deformed as long as we stay in the region of analyticity of the function ϕ_c . At the end we get the following integral representation for the finite sum (16):

$$\sum_{k=1}^{n_s} \phi_c(\lambda_{s,k} - \lambda, \theta) = - \int_{-\infty}^{+\infty} \frac{dx}{2\pi} \phi'_c(x - \lambda, \theta) Z_{L,s}(x) \tag{29}$$

$$\begin{aligned}
& + \lim_{\eta \rightarrow 0^+} 2 \operatorname{Im} \int_{-\infty}^{+\infty} \frac{dx}{2\pi} \phi'_c(x - \lambda, \theta) \log \left[1 + (-1)^\delta \exp[iZ_{L,s}(x + i\eta)] \right] \\
& + \text{border terms.}
\end{aligned}$$

In the following, for notational convenience, we will omit the limit symbol and claim validity of the equations only in the limit $\eta \rightarrow 0^+$.

Notice that in deriving relation (29) we made the fundamental assumption that the BA roots $\lambda_{s,k}$ were positioned on the real line and that real holes were not present. If real holes $h_{s,k}$ are present the equality (29) is not valid anymore. Infact the function (17) will vanish at the real holes $h_{s,k}$ so that the rhs of (29) will contain, beside the contribution coming from the BA roots $\sum \phi_c(\lambda_{s,k} - \lambda, \theta)$, also a contribution coming from the BA holes $\sum \phi_c(h_{s,k} - \lambda, \theta)$.

4 Non-linear integral equation

In this section we will derive a set of coupled non-linear integral equations (NLIE) for the counting functions. Making use of the key result (29) we can reexpress the finite sums that enter in the rhs of (12) in terms of integrals that involve the counting functions:

$$\begin{pmatrix} Z_{L,u} \\ Z_{L,w} \\ Z_{L,v} \end{pmatrix} = -\frac{L}{2} \Phi_1 \begin{pmatrix} 1 \\ 0 \\ 1 \end{pmatrix} + \Phi * \begin{pmatrix} Z_{L,u} \\ Z_{L,w} \\ Z_{L,v} \end{pmatrix} - 2 \operatorname{Im} \Phi * \begin{pmatrix} Q_{L,u} \\ Q_{L,w} \\ Q_{L,v} \end{pmatrix} - \begin{pmatrix} 0 \\ 2\pi\alpha \\ 0 \end{pmatrix}. \quad (30)$$

And we have checked that the border terms vanish. Let us clarify the notation: The symbol $*$ means that in performing the matrix product the ordinary product has to be replaced with the convolution product. We have defined the derivative of (13) as:

$$\Phi_c(x, \theta) \equiv \frac{1}{2\pi} \frac{d}{dx} \phi_c(x, \theta) \quad (31)$$

and introduced the shorthand notation for the non-linear part:

$$Q_{L,s}(x) \equiv \log \left[1 + (-1)^\delta \exp[iZ_{L,s}(x + i\eta)] \right]. \quad (32)$$

The matrix Φ is defined as:

$$\Phi \equiv \begin{pmatrix} \Phi_2 & -\Phi_1 & 0 \\ -\Phi_1 & \Phi_2 & -\Phi_1 \\ 0 & -\Phi_1 & \Phi_2 \end{pmatrix}. \quad (33)$$

In order to solve equation (30) for $Z_{L,s}$ in terms of the non-linear part $Q_{L,s}$ it is convenient to work with the Fourier transform:

$$\begin{pmatrix} \tilde{Z}_{L,u} \\ \tilde{Z}_{L,w} \\ \tilde{Z}_{L,v} \end{pmatrix} = -\frac{L}{2} \tilde{\Phi}_1 (\mathbf{1} - \tilde{\Phi})^{-1} \begin{pmatrix} 1 \\ 0 \\ 1 \end{pmatrix} - 2 \operatorname{Im} (\mathbf{1} - \tilde{\Phi})^{-1} \tilde{\Phi} \begin{pmatrix} \tilde{Q}_{L,u} \\ \tilde{Q}_{L,w} \\ \tilde{Q}_{L,v} \end{pmatrix} \quad (34)$$

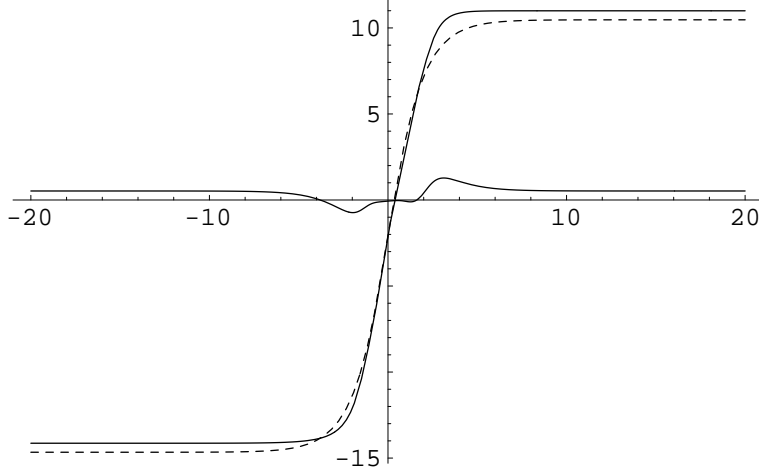


Figure 2: Plot of the terms entering in the second equation of the non-linear system (38). Similar plots hold for the first and the third equation. The parameters of the system are $L = 8$, $n_u = n_w = n_v = L/2$ and $\theta = \alpha = 1/4$. The curve close to the real axis represents the non-linear correction $2 \operatorname{Im} G_{2,s} * Q_{L,s}$ which vanishes in the limit $L \rightarrow \infty$. The dashed line is the bulk term $2\pi L z_w - 2\pi\alpha/(1-\theta)$ and the bold line shows the behaviour of the counting function $Z_{L,w}$.

$$-\delta(p) (\mathbf{1} - \tilde{\Phi})^{-1}(0) \begin{pmatrix} 0 \\ 2\pi\alpha \\ 0 \end{pmatrix}$$

where the Fourier transform and its inverse are defined by:

$$F[\phi](p) \equiv \tilde{\phi}(p) \equiv \int_{-\infty}^{+\infty} e^{-ipx} \phi(x) dx \quad F^{-1}[\tilde{\phi}](x) \equiv \frac{1}{2\pi} \int_{-\infty}^{+\infty} e^{ipx} \tilde{\phi}(p) dp. \quad (35)$$

In particular:

$$\int_{-\infty}^{+\infty} e^{-ipx} \Phi_c(x, \theta) dx = \frac{\sinh(p(c - 1/\theta))}{\sinh(p/\theta)}. \quad (36)$$

We will need the following limit:

$$\tilde{\mathbf{G}}(p, \theta) \equiv -(\mathbf{1} - \tilde{\Phi})^{-1} \tilde{\Phi}, \quad \lim_{p \rightarrow 0} \tilde{\mathbf{G}}(p, \theta) = \frac{1}{4(1-\theta)} \begin{pmatrix} 1-4\theta & -2 & -1 \\ -2 & -4\theta & -2 \\ -1 & -2 & 1-4\theta \end{pmatrix}. \quad (37)$$

Working out the terms in (34) and computing the inverse Fourier transform we get a system of non-linear integral equations (NLIE) for the counting functions:

$$\begin{pmatrix} Z_{L,u} \\ Z_{L,w} \\ Z_{L,v} \end{pmatrix} = 2\pi L \begin{pmatrix} z_u \\ z_w \\ z_v \end{pmatrix} + \lim_{\eta \rightarrow 0^+} 2 \operatorname{Im} \mathbf{G} * \begin{pmatrix} Q_{L,u} \\ Q_{L,w} \\ Q_{L,v} \end{pmatrix} - \frac{\pi\alpha}{(1-\theta)} \begin{pmatrix} 1 \\ 2 \\ 1 \end{pmatrix} \quad (38)$$

where the bulk quantities are given by:

$$z_w(x) = \frac{1}{\pi} \arctan \left(\tanh(\pi x/8) \right) \quad z_u(x) = z_v(x) = \frac{1}{2\pi} \arctan \left(\sqrt{2} \sinh(\pi x/4) \right). \quad (39)$$

We will need their asymptotic behaviour:

$$\lim_{x \rightarrow +\infty} z_{u,v}(x) \sim \frac{1}{4} - \frac{1}{\sqrt{2}\pi} \exp[-\pi x/4] \quad \lim_{x \rightarrow +\infty} z_w(x) \sim \frac{1}{4} - \frac{1}{\pi} \exp[-\pi x/4]. \quad (40)$$

A plot of the various terms entering in the second equation of (38) is shown in figure 2. Similar plots hold for the first and third equation.

5 Integral expression for the free energy

In this section we will derive an integral expression for the finite-size free energy. First we have to express the free energy as the sum of some function evaluated at the BA roots and then applying formula (29) convert the finite sum into an integral. For that purpose notice that for the distribution of the BA roots corresponding to the largest eigenvalue the following equality is satisfied [1]:

$$\prod_{j=1}^{n_u} S_1(u_j, \theta)^{1/2} \prod_{k=1}^{n_v} S_1(v_k, \theta)^{1/2} = \exp[i \pi \alpha] \quad (41)$$

which allows to write the finite-size free energy (3,11) as:

$$f(L) = -\frac{1}{L} \left[\log 2 + \log \cos(2 \pi \alpha + s_2) + \frac{1}{2} s_1 \right] \quad (42)$$

where the finite sums s_1 and s_2 are defined by:

$$\begin{aligned} s_1 &= \sum_{m=1}^{n_w} \log \left(\cos^2 \pi \theta + \sin^2 \pi \theta \coth^2 \frac{\pi \theta w_m}{2} \right) \\ s_2 &= \sum_{m=1}^{n_w} \arctan \left(\tan \pi \theta \coth \left(\frac{\pi \theta w_m}{2} \right) \right). \end{aligned} \quad (43)$$

We will show in the Appendix that only s_1 contributes to the value of the central charge. In the sequel we will manipulate the sum s_1 in order to extract the exact value of the central charge. The function entering in the sum s_1 (43) and its derivative are defined by:

$$\varphi(w) \equiv \log \left(\cos^2 \pi \theta + \sin^2 \pi \theta \coth^2 \frac{\pi \theta w}{2} \right) \quad W(w) \equiv \frac{d}{dw} \varphi(w). \quad (44)$$

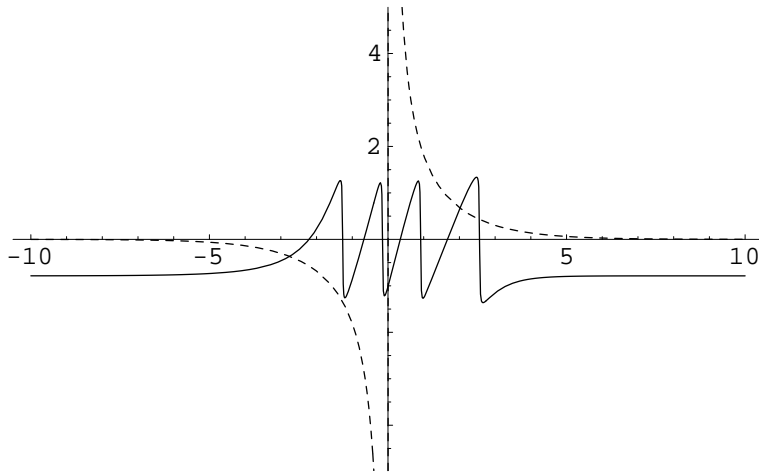


Figure 3: Plot of the function $H_w(x)$ (dashed line) and of the oscillating non-linear term $\text{Im} \log[1 + \exp[i Z_{L,w}(x + i\eta)]]$. We refer to a system of size $L = 8$, phases $\alpha = \theta = 1/4$ and parameter $\eta = 0.01$. At the four BA roots w_j the non-linear term exhibits a rapid variation.

At this point remember that in deriving the key result (29) which allows the conversion of a finite sum into an integral we made the fundamental assumption that the function entering in the sum was analytic in the region delimited by the contour integral. And moreover that the BA roots were located inside that region. The analyticity requirement is not satisfied in this particular case because $\varphi(w)$ (44) is not analytic at the origin. To overcome the problem we apply the formalism of section 3 taking as contour line two boxes, one positioned on the right and the other on the left side of the origin, that contain all the w_j roots. This is illustrated in figure 4 (b). Now, besides the border terms at infinity, there will be also border terms at the origin. They are studied in the Appendix. The finite sum s_1 in integral form becomes:

$$\begin{aligned}
 s_1 &= -\text{Vp} \int_{-\infty}^{+\infty} \frac{dx}{2\pi} W(x) Z_{L,w}(x) \\
 &+ 2 \text{Im Vp} \int_{-\infty}^{+\infty} \frac{dx}{2\pi} W(x) \log \left[1 + \exp[i Z_{L,w}(x + i\eta)] \right] + \text{border terms}
 \end{aligned}
 \tag{45}$$

where Vp denotes the principal value. The first term on the rhs of (45) can be rewritten substituting the expression for the counting function given by the non-linear integral equation (38). In order to perform the calculations it is convenient to apply Parseval formula so that $W(x)$, $Z_{L,w}(x)$ and the non-linear term can be replaced by their respective Fourier transform, and then make use of the expression (34) for the counting function. Performing the calculations in the Fourier space and then applying again Parseval formula

via the inverse Fourier transform we get the following integral expression for the sum s_1 :

$$\begin{aligned}
s_1 = & -L \text{Vp} \int_{-\infty}^{+\infty} dx W(x) z_w(x) + \frac{\alpha}{1-\theta} \text{Vp} \int_{-\infty}^{+\infty} dx W(x) \\
& + 2 \text{Im} \text{Vp} \int_{-\infty}^{+\infty} \frac{dx}{2\pi} H_u(x) \log \left[1 + \exp[i Z_{L,u}(x + i\eta)] \right] \\
& - 2 \text{Im} \text{Vp} \int_{-\infty}^{+\infty} \frac{dx}{2\pi} H_w(x) \log \left[1 + \exp[i Z_{L,w}(x + i\eta)] \right] \\
& + 2 \text{Im} \text{Vp} \int_{-\infty}^{+\infty} \frac{dx}{2\pi} H_v(x) \log \left[1 + \exp[i Z_{L,v}(x + i\eta)] \right] \\
& + \text{border terms}
\end{aligned} \tag{46}$$

where the functions $H_s(x)$ are given by:

$$H_u(x) = H_v(x) = -\frac{\pi}{\sqrt{2}} \frac{\sinh(\pi x/4)}{\cosh(\pi x/2)} \quad H_w(x) = \frac{\pi}{2} \text{csch}(\pi x/4). \tag{47}$$

It is remarkable to notice that the functions $H_s(x)$ do not depend on the parameter θ . The θ dependence is carried by the logarithmic factors which contain the counting functions. Notice that the rhs of (46) gives an exact expression for the finite-size sum s_1 in terms of the finite-size counting functions $Z_{L,s}$.

Let us examine the various terms that appear in rhs of (46). The first term is the dominant one and is responsible for the bulk free energy. The second one comes from the constant part in the NLIE (38). It gives a contribution to the finite-size free energy density which scales like $1/L$. Its contribution exactly cancels with a same contribution coming from the border terms. The last three integrals, which exhibit a non-linear dependence on the counting functions, will generate the higher order corrections. A plot of the function $H_w(x)$ and of the non-linear part $\text{Im} \log[1 + \exp[i Z_{L,w}(x + i\eta)]]$ is shown in figure 3. The non-linear part exhibits rapid jumps at the BA roots w_j . Due to the rapid oscillations, it is responsible for the vanishing of the integral in the limit $L \rightarrow \infty$. In the next section we are going to extract, from these integrals, the corrections of order $1/L^2$ which determine the value of the central charge.

6 The central charge

In order to compute the central charge we have to manipulate the NLIE (38) and the expressions (42) and (46) for the free energy. We make the following change of variable [30]:

$$x = 4(\mu + \log L)/\pi \tag{48}$$

which depends on the size of the system, and introduce the functions:

$$\begin{aligned} F_{L,s}(x) &\equiv \exp[i Z_{L,s}(x)] \\ F_{+,s}(\mu) &\equiv \lim_{L \rightarrow +\infty} F_{L,s}(4(\mu + \log L)/\pi) \quad Q_{+,s}(\mu) \equiv 2 \operatorname{Im} \log[1 + F_{+,s}(\mu + i\eta)]. \end{aligned} \quad (49)$$

Making use of the asymptotics (40) we see that in the limit $L \rightarrow +\infty$ the NLIE (38) reduces to:

$$\begin{aligned} -i \log \begin{bmatrix} F_{+,u}(\mu) \\ F_{+,w}(\mu) \\ F_{+,v}(\mu) \end{bmatrix} &= - \begin{pmatrix} \sqrt{2} \\ 2 \\ \sqrt{2} \end{pmatrix} e^{-\mu} - \frac{\pi \alpha}{(1-\theta)} \begin{pmatrix} 1 \\ 2 \\ 1 \end{pmatrix} \\ &+ 2 \operatorname{Im} \int_{-\infty}^{+\infty} d\mu' \mathbf{G}(\mu' - \mu) \log \begin{bmatrix} 1 + F_{+,u}(\mu' + i\eta) \\ 1 + F_{+,w}(\mu' + i\eta) \\ 1 + F_{+,v}(\mu' + i\eta) \end{bmatrix}. \end{aligned} \quad (50)$$

This is a non-linear integral equation for the unknown functions $F_{+,s}(\mu)$. The dependence on the size of the system L has dropped. In particular comparing with (38) we see that the terms of order L has been reduced to exponentials. We show now that performing the change of variable (48) in the expression for the free energy it is possible to extract the correction of order $1/L^2$. First notice that the functions $H_s(x)$ that enter in the integrals (46) have the following asymptotic behaviour:

$$\lim_{x \rightarrow +\infty} H_{u,v}(x) \sim -\frac{\pi}{\sqrt{2}} \exp[-\pi x/4] \quad \lim_{x \rightarrow +\infty} H_w(x) \sim \pi \exp[-\pi x/4]. \quad (51)$$

In the new variable μ the leading terms are:

$$\lim_{L \rightarrow +\infty} H_{u,v}(4(\mu + \log L)/\pi) \sim -\frac{\pi}{\sqrt{2}L} e^{-\mu} \quad \lim_{L \rightarrow +\infty} H_w(4(\mu + \log L)/\pi) \sim \frac{\pi}{L} e^{-\mu}. \quad (52)$$

so that the expression for the free energy (42, 46) reduces to:

$$f(L) \sim f(\infty) + \frac{C_+ + C_-}{2\pi L^2} + o(1/L^2) \quad (53)$$

where the constant C_+ is defined in terms of integrals of the functions $F_{+,s}(\mu)$:

$$\begin{aligned} C_+ &= 2 \operatorname{Im} \int_{-\infty}^{+\infty} d\mu \sqrt{2} e^{-\mu} \log[1 + F_{+,u}(\mu + i\eta)] \\ &+ 2 \operatorname{Im} \int_{-\infty}^{+\infty} d\mu 2 e^{-\mu} \log[1 + F_{+,w}(\mu + i\eta)] \\ &+ 2 \operatorname{Im} \int_{-\infty}^{+\infty} d\mu \sqrt{2} e^{-\mu} \log[1 + F_{+,v}(\mu + i\eta)]. \end{aligned} \quad (54)$$

Notice that the effect of the change of variable (48) on the last three integrals of (46) is twofold: It shifts the oscillating terms so that only one of the two tails of the functions H_s will contribute to the integral, and in the limit $L \rightarrow +\infty$ it extracts from the function $H_s(4(\mu + \log L)/\pi)$ the leading term $e^{-\mu}/L$. In order to compute the contribution to the finite-size corrections coming from the other tail we have to perform the change of variable $x = 4(\mu - \log L)/\pi$. We denote the two contributions by C_+ and C_- .

Fortunately, it is not necessary to solve the non-linear integral equation (50) in order to calculate the constant C_+ . In fact we can make use of the following formula [34]:

$$\begin{aligned}
C_+ &= -2 \operatorname{Re} \sum_s \int_{\Gamma_s} \frac{du}{u} \log(1+u) \\
&\quad - \frac{1}{2} \sum_{r,s} Q_{+,r}(+\infty) Q_{+,s}(+\infty) \int_{-\infty}^{+\infty} dx G_{r,s}(x) \\
&\quad + \frac{1}{2} \sum_{r,s} Q_{+,r}(-\infty) Q_{+,s}(-\infty) \int_{-\infty}^{+\infty} dx G_{r,s}(x)
\end{aligned} \tag{55}$$

where Γ_s is an arbitrary line of integration in the complex plane connecting $F_{+,s}(-\infty + i0^+)$ to $F_{+,s}(+\infty + i0^+)$ and avoiding the logarithmic cut $(-\infty, -1]$. This is the multicomponent generalization of the lemma proved in [31]. For completeness we reproduce the proof in the Appendix. The limit quantities that enter in the previous formula have the following values:

$$\begin{aligned}
F_{+,s}(-\infty + i0^+) &= 0 & Q_{+,s}(-\infty) &= 0 & s &= u, w, v \\
F_{+,s}(+\infty + i0^+) &= 1 & Q_{+,s}(+\infty) &= 0 & s &= u, v \\
F_{+,w}(+\infty + i0^+) &= \exp[-2i\pi\alpha] & Q_{+,w}(+\infty) &= -2\pi\alpha.
\end{aligned} \tag{56}$$

The integrals involving $G_{r,s}$ can be calculated with the help of the Fourier transform (37). Summing all the contributions, C_+ becomes:

$$C_+ = \left[-\frac{\pi^2}{6}\right]_u + \left[-\frac{\pi^2}{6} + \frac{4\pi^2\alpha^2}{2}\right]_w + \left[-\frac{\pi^2}{6}\right]_v + \frac{4\pi^2\alpha^2}{2} \frac{\theta}{1-\theta} = -\frac{\pi^2}{6} \left(3 - \frac{12\alpha^2}{1-\theta}\right). \tag{57}$$

The three square brackets refer to the dilogarithm part in formula (55) for the three families of BA roots, respectively u , w and v . The dilogarithms are worked out using the following formula:

$$-2 \operatorname{Re} \int_0^{e^{i\omega}} \frac{du}{u} \log(1+u) = -\frac{\pi^2}{6} + \frac{\omega^2}{2}. \tag{58}$$

The same result holds for C_- so that the central charge (4) is given by:

$$c = 3 - \frac{12\alpha^2}{1-\theta} \tag{59}$$

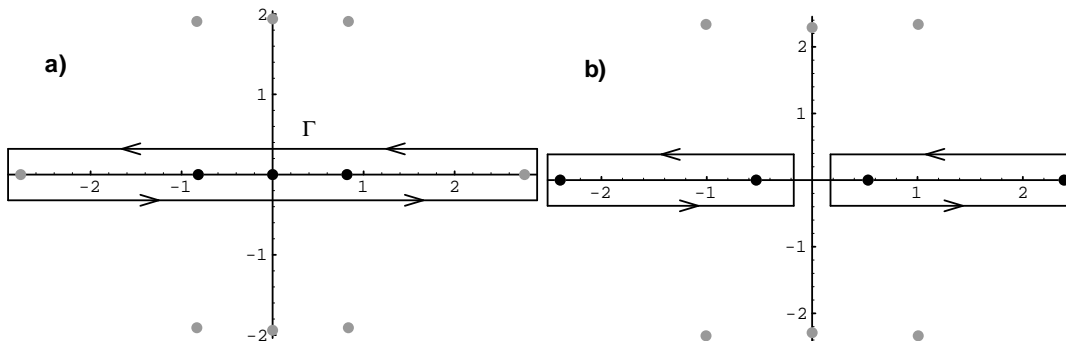


Figure 4: Arrangement of the roots (black circles) and of the holes (grey circles) in the complex plane. a) The u -family. b) The w -family. The parameters are: $L = 8$, $n_v = n_w = 8$, $n_u = 7$, $\alpha = \theta \rightarrow 0$. The u -family has two real holes. The contour lines which encircles the Bethe ansatz roots are shown. a) Notice that for the u -family the contour line encircles also the two real holes. b) In deriving an integral expression for the free energy we avoid the origin splitting the contour line into two boxes.

which is in agreement with the result found in [4, 3]. In particular we see that for the four-coloring problem [4, 11, 12], which corresponds to the choice $\theta = \alpha = 0$ the central charge is $c = 3$. For the double Hamiltonian walk ($\theta = \alpha = 1/2$) [4, 10] the central charge becomes negative $c = -3$. In general, the shift of the value of the central charge due to the presence of the seam has been investigated in [18, 20].

7 The excitations

The largest eigenvalue of the transfer matrix lies in the sector $n_u = n_v = n_w = L/2$ and corresponds to roots distributed on the real axis in such a way that the close packing constraint is satisfied [1]:

$$Z_{L,s}(\lambda_{s,k+1}) - Z_{L,s}(\lambda_{s,k}) = 2\pi \quad k = 1, \dots, n_s - 1 \quad s = u, w, v \quad (60)$$

Subdominant eigenvalues of the transfer matrix can be constructed by perturbing this distribution [22]. One way of doing that (particle-hole excitations) is to insert real holes $h_{s,k}$ that will break the close packing of the real roots. Another family of excitations (charge excitations) can be constructed by varying the parameters n_u , n_w and n_v that enter in the BAE (8-10). A third family of excitations (umklapp processes) can be constructed shifting the ground state distribution of the roots. To obtain this last excitation we have to replace in (14) the integer numbers $I_{s,k}$, that characterize the distribution of the roots corresponding to the largest eigenvalue, by $I_{s,k} \rightarrow I_{s,k} \pm 1$ for $k = 1, \dots, n_s$.

In the following we are going to compute analytically, with the help of formula (5), the scaling dimension Δ_i associated with the excitation in which n_u is decreased by one.

We checked numerically that for the distribution of the BA roots associated with this particular excitation relation (41) is satisfied so that the finite-size energy associated with the excited eigenvalue $\Lambda_i(L)$ is given by:

$$\log \Lambda_i(L) = \log 2 + \log \cos(2 \pi \alpha + s_2) + \frac{1}{2} s_1 \quad (61)$$

where the sums s_1 and s_2 are defined by (43). We show in the Appendix that also in this case the contribution to the value of the scaling dimension comes exclusively from the sum s_1 . Thus, the machinery developed in section 6 for the calculation of the central charge can be applied, with small changes, also in this case. Solving numerically the BA equations for the excited state we see that two real holes appear for the u -family. This is shown in figure 4 (a). There are no real holes for the other two families of roots. To denote the position of the real u -holes we introduce the positive real numbers h_1 for the hole located on the positive real axis and h_2 for the hole on the negative axis. Also in this case, following the steps of section 4, we can write a non-linear integral equation for the counting function. For that notice that the sums, entering in the counting functions (12), run over the BA roots. On the other hand the contour integral is a box centered around the origin and extending from $-\infty$ to $+\infty$, so that it will encircle also the two holes located at the border of the u -roots (see figure 4 (a)). At the end their contribution must be subtracted. The analog of Eq. (30) becomes:

$$\begin{aligned} \begin{pmatrix} Z_{L,u}(x) \\ Z_{L,w}(x) \\ Z_{L,v}(x) \end{pmatrix} &= -\frac{L}{2} \Phi_1 \begin{pmatrix} 1 \\ 0 \\ 1 \end{pmatrix} + \Phi * \begin{pmatrix} Z_{L,u} \\ Z_{L,w} \\ Z_{L,v} \end{pmatrix} - \begin{pmatrix} 0 \\ 2 \pi \alpha \\ 0 \end{pmatrix} \\ &+ \begin{pmatrix} \phi_2(h_1 - x) + \phi_2(-h_2 - x) \\ -\phi_1(h_1 - x) - \phi_1(-h_2 - x) \\ 0 \end{pmatrix} \\ &- 2 \operatorname{Im} \int_{-\infty}^{+\infty} dx' \mathbf{G}(x' - x) \log \begin{bmatrix} 1 - \exp[i Z_{L,u}(x' + i \eta)] \\ 1 + \exp[i Z_{L,w}(x' + i \eta)] \\ 1 + \exp[i Z_{L,v}(x' + i \eta)] \end{bmatrix}. \end{aligned} \quad (62)$$

Notice that in the non-linear term of (62) there is a minus sign in front of $\exp[i Z_{L,u}]$. This is because for the excited state we are investigating the counting function $Z_{L,u}$ evaluated at the BA roots and holes is an even multiple of π . With this change of sign it turns out that the function $(1 - \exp[i Z_{L,u}])$ has a zero of order one at the BA roots and holes, a necessary condition to apply the machinery developed in section 3. Repeating the calculations of section 4 we can write the analogue of (38) for the particular excited state we are investigating:

$$\begin{pmatrix} Z_{L,u}(x) \\ Z_{L,w}(x) \\ Z_{L,v}(x) \end{pmatrix} = 2 \pi L \begin{pmatrix} z_u \\ z_w \\ z_v \end{pmatrix} - \frac{\pi \alpha}{(1 - \theta)} \begin{pmatrix} 1 \\ 2 \\ 1 \end{pmatrix} + \begin{pmatrix} S_u(x + h_2) + S_u(x - h_1) \\ S_w(x + h_2) + S_w(x - h_1) \\ S_v(x + h_2) + S_v(x - h_1) \end{pmatrix}$$

$$+2 \operatorname{Im} \int_{-\infty}^{+\infty} dx' \mathbf{G}(x' - x) \log \begin{bmatrix} 1 - \exp[i Z_{L,u}(x' + i\eta)] \\ 1 + \exp[i Z_{L,w}(x' + i\eta)] \\ 1 + \exp[i Z_{L,v}(x' + i\eta)] \end{bmatrix} \quad (63)$$

where the vector \mathbf{S} can be expressed in terms of the inverse Fourier transform of the matrix $\tilde{\mathbf{G}}(p, \theta)$ (37):

$$\begin{pmatrix} S_u(x) \\ S_w(x) \\ S_v(x) \end{pmatrix} = \int_{-\infty}^{+\infty} dp \frac{\sin xp}{p} \begin{pmatrix} \tilde{G}_{11} \\ \tilde{G}_{21} \\ \tilde{G}_{31} \end{pmatrix}. \quad (64)$$

In particular it turns out that the derivative of \mathbf{S} is related to \mathbf{G} :

$$\frac{d}{dx} \begin{pmatrix} S_u(x) \\ S_w(x) \\ S_v(x) \end{pmatrix} = 2\pi \begin{pmatrix} G_{11}(x) \\ G_{21}(x) \\ G_{31}(x) \end{pmatrix}. \quad (65)$$

From expression (64) and (37) we read the limit values of \mathbf{S} :

$$\lim_{x \rightarrow \pm\infty} \begin{pmatrix} S_u(x) \\ S_w(x) \\ S_v(x) \end{pmatrix} = \pm\pi \begin{pmatrix} (1 - 4\theta)/(4 - 4\theta) \\ 1/(-2 + 2\theta) \\ 1/(-4 + 4\theta) \end{pmatrix}. \quad (66)$$

Performing the change of variable (48) and taking the limit $L \rightarrow +\infty$, equation (63) reduces to:

$$\begin{aligned} -i \log \begin{bmatrix} F_{+,u}(\mu) \\ F_{+,w}(\mu) \\ F_{+,v}(\mu) \end{bmatrix} &= - \begin{pmatrix} \sqrt{2} \\ 2 \\ \sqrt{2} \end{pmatrix} e^{-\mu} - \frac{\pi \alpha}{(1 - \theta)} \begin{pmatrix} 1 \\ 2 \\ 1 \end{pmatrix} \\ &+ \pi \begin{pmatrix} (1 - 4\theta)/(4 - 4\theta) \\ 1/(-2 + 2\theta) \\ 1/(-4 + 4\theta) \end{pmatrix} + \begin{pmatrix} S_u(\mu - \mu_{h_1}) \\ S_w(\mu - \mu_{h_1}) \\ S_v(\mu - \mu_{h_1}) \end{pmatrix} \\ &+ 2 \operatorname{Im} \int_{-\infty}^{+\infty} d\mu' \mathbf{G}(\mu' - \mu) \log \begin{bmatrix} 1 - F_{+,u}(\mu' + i\eta) \\ 1 + F_{+,w}(\mu' + i\eta) \\ 1 + F_{+,v}(\mu' + i\eta) \end{bmatrix} \end{aligned} \quad (67)$$

which is the analogue of (50) for the excited state. We will need the following limit values:

$$\begin{aligned} F_{+,s}(-\infty + i0) &= 0 & Q_{+,s}(-\infty) &= 0 & s &= u, w, v \\ F_{+,u}(+\infty) &= \exp[i\pi(1 - 2\theta)] & Q_{+,u}(+\infty) &= -2\pi\theta \\ F_{+,w}(+\infty) &= \exp[i\pi(-1 - 2\alpha + \theta)] & Q_{+,w}(+\infty) &= \pi(-1 - 2\alpha + \theta) \\ F_{+,v}(+\infty) &= 1 & Q_{+,v}(+\infty) &= 0. \end{aligned} \quad (68)$$

The excitation we are studying modifies also the integral expression for the finite-size free energy. In particular in the integral expression for the sum s_1 (46) the following extra term will appear:

$$\int_{-\infty}^{+\infty} \frac{dx}{2\pi} W(x) (S_w(x+h_2) + S_w(x-h_1)). \quad (69)$$

In the following we will compute the contribution to the finite-size correction coming from the hole located at position h_1 . Similar calculations hold for the hole positioned at $-h_2$. Working out the integral we obtain:

$$\int_{-\infty}^{+\infty} \frac{dx}{2\pi} W(x) S_w(x-h_1) = \log \left(\frac{\cosh(h_1 \pi/4) + 1/\sqrt{2}}{\cosh(h_1 \pi/4) - 1/\sqrt{2}} \right) \quad (70)$$

which has the following asymptotic behaviour:

$$\lim_{h_1 \rightarrow +\infty} \log \left(\frac{\cosh(h_1 \pi/4) + 1/\sqrt{2}}{\cosh(h_1 \pi/4) - 1/\sqrt{2}} \right) \sim 2\sqrt{2} \exp[-h_1 \pi/4]. \quad (71)$$

Following the steps of section 6 we see that, in the limit $L \rightarrow +\infty$, the finite-size energy of the excited state reduces to:

$$\log \Lambda_i(L) = \text{bulk} + \frac{C_+ + C_-}{2\pi L} + o(1/L) \quad (72)$$

where the constant C_+ is now given by:

$$\begin{aligned} C_+ = & -2\pi\sqrt{2} \exp[-\mu_{h_1}] \\ & -2 \operatorname{Im} \int_{-\infty}^{+\infty} d\mu \sqrt{2} e^{-\mu} \log[1 - F_{+,u}(\mu + i\eta)] \\ & -2 \operatorname{Im} \int_{-\infty}^{+\infty} d\mu 2e^{-\mu} \log[1 + F_{+,w}(\mu + i\eta)] \\ & -2 \operatorname{Im} \int_{-\infty}^{+\infty} d\mu \sqrt{2} e^{-\mu} \log[1 + F_{+,w}(\mu + i\eta)]. \end{aligned} \quad (73)$$

The bulk term in (72) coincides with the bulk term of the ground state eigenvalue (53). The dominant finite-size correction has a different structure. In fact comparing (73) with (54) we see that there is an extra contribution $-2\pi\sqrt{2} \exp[-\mu_{h_1}]$ due to the presence of the hole positioned at μ_{h_1} and there is a minus sign in front of $F_{+,u}$. A similar expression can be derived for C_- performing the change of variable $x = 4(\mu - \log L)/\pi$ which selects the hole located at $-\mu_{h_2}$. Now we are going to rewrite (73) in a fashion that allows the application of formula (55). For that notice that the hole located at μ_{h_1} solves the first

equation of the system (67) for some integer number I_{h_1} :

$$\begin{aligned}
2\pi I_{h_1} &= -\sqrt{2} \exp[-\mu_{h_1}] - \frac{\pi \alpha}{(1-\theta)} + \frac{\pi(1-4\theta)}{4(1-\theta)} + S_u(0) \\
&+ 2 \operatorname{Im} \int_{-\infty}^{+\infty} \frac{d\mu}{2\pi} \frac{d}{d\mu} S_u(\mu - \mu_{h_1}) \log[1 - F_{+,u}(\mu + i\eta)] \\
&+ 2 \operatorname{Im} \int_{-\infty}^{+\infty} \frac{d\mu}{2\pi} \frac{d}{d\mu} S_w(\mu - \mu_{h_1}) \log[1 + F_{+,w}(\mu + i\eta)] \\
&+ 2 \operatorname{Im} \int_{-\infty}^{+\infty} \frac{d\mu}{2\pi} \frac{d}{d\mu} S_v(\mu - \mu_{h_1}) \log[1 + F_{+,v}(\mu + i\eta)]
\end{aligned} \tag{74}$$

where according to (64) $S_u(0) = 0$. Now, substituting the expression for the exponential, given by relation (74) into the rhs of (73) we get the following expression for C_+ :

$$\begin{aligned}
C_+ &= 4\pi^2 I_{h_1} + \frac{2\pi^2 \alpha}{1-\theta} - \frac{\pi^2(1-4\theta)}{2(1-\theta)} \\
&- 2 \operatorname{Im} \int_{-\infty}^{+\infty} d\mu \left[\sqrt{2} e^{-\mu} + \frac{d}{d\mu} S_u(\mu - \mu_{h_1}) \right] \log[1 - F_{+,u}(\mu + i\eta)] \\
&- 2 \operatorname{Im} \int_{-\infty}^{+\infty} d\mu \left[2e^{-\mu} + \frac{d}{d\mu} S_w(\mu - \mu_{h_1}) \right] \log[1 + F_{+,w}(\mu + i\eta)] \\
&- 2 \operatorname{Im} \int_{-\infty}^{+\infty} d\mu \left[\sqrt{2} e^{-\mu} + \frac{d}{d\mu} S_v(\mu - \mu_{h_1}) \right] \log[1 + F_{+,v}(\mu + i\eta)].
\end{aligned} \tag{75}$$

Notice that the expression in square brackets is the derivative of the first four terms on the rhs of (67) so that we are in the position to apply formula (55). Showing all the terms:

$$\begin{aligned}
C_+ &= 4\pi^2 I_{h_1} + \frac{2\pi^2 \alpha}{1-\theta} - \frac{\pi^2(1-4\theta)}{2(1-\theta)} \\
&- \pi^2 \left(\left[\frac{1}{3} + \frac{(1-2\theta)^2}{2} - (1-2\theta) \right]_u + \left[-\frac{1}{6} + \frac{(-1-2\alpha+\theta)^2}{2} \right]_w + \left[-\frac{1}{6} \right]_v + q \right).
\end{aligned} \tag{76}$$

For C_- we obtain the same expression with I_{h_1} replaced by I_{h_2} . The three square brackets refer to the dilogarithm part in formula (55) for the three family of BA roots, respectively u , w and v . The dilogarithms are worked out using formula (58) and the limit values (68). In order to compute the contribution coming from the u -term we make use of the formula:

$$-2 \operatorname{Re} \int_0^{e^{i\omega}} \frac{du}{u} \log(1-u) = \frac{\pi^2}{3} + \frac{\omega^2}{2} - \pi\omega.$$

The term q in the expression (76) gives the contribution coming from the non-dilogarithm part of formula (55). Working out we find:

$$q = \frac{\theta(3 + 4\alpha^2 + 8\alpha - 4\alpha\theta - 5\theta + 5\theta^2)}{2(1-\theta)} \tag{77}$$

We have all the ingredients to apply formula (5). Substituting the values of C_- and C_+ in (72) and reminding that the central charge is given by (59) after some algebra we get simple expressions for the scaling dimensions:

$$\Delta_+ = -I_{h_1} + \frac{1-\theta}{4} \quad \Delta_- = -I_{h_2} + \frac{1-\theta}{4} \quad \Delta \equiv \Delta_+ + \Delta_- = \frac{1-\theta}{2} \quad (78)$$

where the α dependence has dropped. From numerical calculation we see that the excitation under investigation corresponds to the choice $I_{h_1} = I_{h_2} = 0$.

From this result we can compute the scaling dimension corresponding to one black and one grey string propagating between two points on the lattice [4]. Call $G_1(r)$ the two string correlation function associated with defects configurations where a single oriented black loop segment and a single oriented grey loop segment propagate from a vertex located at the origin to a vertex positioned r rows above it. If we denote by ϕ the operator which creates the defect, the correlation function, in the transfer matrix formalism is given by:

$$\begin{aligned} G_1(r) &= \langle \phi(r)\phi(0) \rangle = \lim_{N \rightarrow \infty} \frac{1}{Z} \text{Tr} \mathbf{T}_{0,0,0}^{N-r} \phi(r) \mathbf{T}_{-1,0,0}^r \phi(0) \\ &= \sum_n e^{-(E_n(L) - E_0(L))r} \langle 0 | \phi(r) | n \rangle \langle n | \phi(0) | 0 \rangle \end{aligned} \quad (79)$$

where $\mathbf{T}_{0,0,0}$ is the block of the transfer matrix corresponding to the ground state sector and $\mathbf{T}_{-1,0,0}$ is the block corresponding to the excited sector in which the number of u particles is decreased by one. Notice that the sum runs over the eigenvalues $e^{-E_n(L)}$ of $\mathbf{T}_{-1,0,0}$ and $e^{-E_0(L)}$ is the largest eigenvalue of the transfer matrix. In the limit $r \gg 1$ the correlation exhibits, in the cylindrical geometry, an exponential decay:

$$G_1(r) \sim e^{-(E_1 - E_0)r} \quad (80)$$

where $e^{-E_1(L)}$ is the largest eigenvalue of the matrix $\mathbf{T}_{-1,0,0}$. In the bulk ($L \rightarrow \infty$) the correlator exhibits a power law behaviour:

$$G_1(r) \sim \frac{1}{r^{2x_1}}. \quad (81)$$

If the model is conformally invariant the energy gap and the critical exponent can be related via the formula (see also formula (5)):

$$x_1 = \lim_{L \rightarrow \infty} \frac{L}{2\pi} (E_1(L) - E_0(L)). \quad (82)$$

It is important to notice that since $\mathbf{T}_{-1,0,0}^r$ generates the configurations in which a black and a grey string run from the first to the r th row of the cylinder, black and grey winding loops are forbidden inside this region so that there is no need to introduce the seam in order to assign them the right fugacity [13, 27]. Moreover an eventual seam would associate

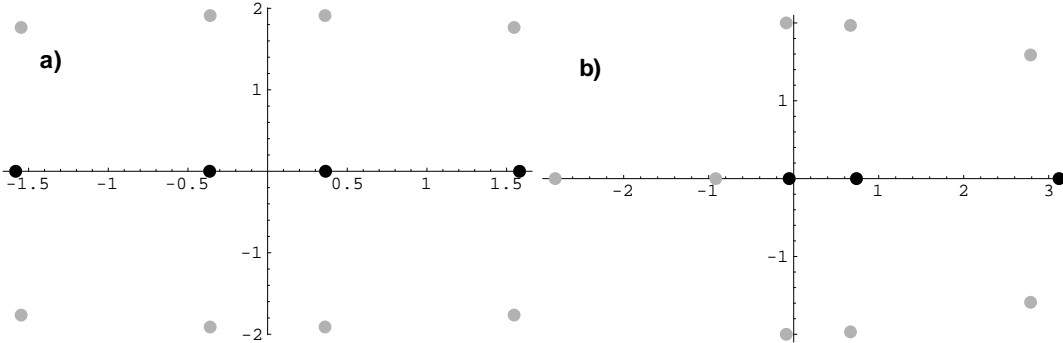


Figure 5: Arrangement of the roots (black circles) and the holes (grey circle) in the complex plane for the u -family. a) Arrangement corresponding to the ground state. The parameters are: $L = 8$, $n_u = n_v = n_w = 4$, $\alpha = \theta = 0$. Notice that the ground state possesses complex holes. b) Arrangement corresponding to the excitation labelled by $\mathbf{m} = (-1, 0, 0)$ and $\mathbf{e} = (1, 0, 0)$. Notice that the charge excitation $\mathbf{m} = (-1, 0, 0)$ generates two real holes at the border of the Fermi sea (see figure 4 (a)). The umklapp process $\mathbf{e} = (1, 0, 0)$ shifts all the root distribution to the right.

a phase, to loops spiralling around the cylinder, proportional to the winding number. Performing the calculation that lead to (78) with $\alpha = \theta$ for the largest eigenvalue and $\alpha = 0$ for the subdominant one we get for the exponent governing the two string correlation function:

$$x_1 = \frac{1 - \theta}{2} - \frac{\theta^2}{1 - \theta} \quad (83)$$

in agreement with the result found in [4] via the field theory. Notice that the second term in the rhs of (83) is 1/12 of the shift of the central charge (see the formula (59) for the central charge).

8 Numerics

In the previous section we have shown in detail how to compute analytically the scaling dimension associated with the excitation in which the parameter n_u is decreased by one. In general, an excitation will be characterized by a particular arrangement of holes and roots in the complex plane. If the arrangement is known the corresponding scaling dimension can be calculated going through the machinery that we have described. In this section we are going to study numerically a larger set of excitations.

To classify the excitations in a compact manner we introduce three vectors $\mathbf{e} = (e_u, e_w, e_v)$, $\mathbf{m} = (m_u, m_w, m_v)$, $\mathbf{I}^\pm = (I_u^\pm, I_w^\pm, I_v^\pm)$. The components of \mathbf{m} are integer numbers which count the change of the “number of particles” in the excited state with respect to the ground state. The components of \mathbf{e} count the total number of transitions

of the “particles” from one side to the other of the three Fermi seas. The non-negative integers I_s^\pm describe excitations in the vicinity of the Fermi surfaces. They count the number of holes that are generated by moving the roots, positioned at the Fermi surfaces, to the next vacant positions. As example, figure 5 shows the arrangement of holes and roots corresponding to the excitation labeled by $\mathbf{m} = (-1, 0, 0)$, $\mathbf{e} = (1, 0, 0)$ and $\mathbf{I}^\pm = (0, 0, 0)$ for a system of size $L = 8$.

Table 1 shows a set of charge excitations labelled by the vector \mathbf{m} . The scaling dimensions have been estimated by solving numerically the BA equations for systems of increasing size and making use of formula (5). Notice that in applying formula (5) the largest and the subdominant eigenvalues were computed keeping the value of α constant and not varying it as in the derivation of (83). From the data we see that the scaling dimensions do not exhibit a dependence on α . The data for $\mathbf{m} = (-1, 0, -1)$ and $\mathbf{m} = (-1, 0, +1)$ merit a special comment. Solving numerically the BA equations for a generic value of θ and setting $\alpha = 0$ we see that two particles at the border of the w -family go to infinity. Specifying the value $w_l = \pm\infty$ in (10) and observing that for the function (7) $\lim_{x \rightarrow \pm\infty} S_c(x, \theta) = -\exp[\mp i \pi \theta c]$ it follows that (10) is satisfied only for $\alpha = 0$. Thus the excitations $\mathbf{m} = (-1, 0, -1)$ and $\mathbf{m} = (-1, 0, +1)$ we have founded only for $\alpha = 0$.

Table 3 shows the scaling dimensions for a set of excitations constructed perturbing the ground state by a combination of charge excitations labelled by \mathbf{m} with umklapp processes labelled by \mathbf{e} . We have checked that for this set of excitations in which the umklapp is involved the scaling dimensions exhibit a dependence on α .

Table 2 shows the scaling dimensions for a set of excitations constructed combining charge excitations \mathbf{m} with particle-hole excitations labelled by \mathbf{I}^\pm . In order to construct the particle-hole excitations we insert a hole at the very end of the Fermi sea. Notice that there are three Fermi seas, one for each type of particles, and each Fermi sea has two surfaces that can be perturbed independently. We distinguish among the two surfaces using an upper index for the vector \mathbf{I}^\pm . From the data we see that the scaling dimensions for this class of excitations do not depend on the phase α . Notice that the scaling dimension for the excitation labelled by $\mathbf{m} = (-1, 0, 0)$ and $\mathbf{I}^+ = (1, 0, 0)$ can be calculated analytically setting in formula (78) $I_{h_1} = -1$ and $I_{h_2} = 0$

The set of excitations shown in table 1 and 3 does not cover all the possibilities. In fact we did not succeed in finding the excitation labelled by $\mathbf{e} = (+1, +1, 0)$ and the one labelled by $\mathbf{m} = (+1, -1, 0)$. The numerical data, of the low-lying excitations we could construct, suggest that the scaling dimensions Δ , are described by the formula:

$$\Delta(\mathbf{m}, \mathbf{e}, \mathbf{I}^\pm, \theta) = \frac{1-\theta}{4} \mathbf{m}^t \mathbf{C} \mathbf{m} + \frac{1}{1-\theta} \mathbf{e}^t \mathbf{C}^{-1} (\mathbf{e} - \mathbf{e}_0) + \sum_s I_s^+ + \sum_s I_s^- \quad (84)$$

where the background charge is given by $\mathbf{e}_0 = (0, 2\alpha, 0)$, and \mathbf{C} is the Cartan matrix of sl_4 :

$$\mathbf{C} = \begin{pmatrix} 2 & -1 & 0 \\ -1 & 2 & -1 \\ 0 & -1 & 2 \end{pmatrix} \quad (85)$$

\mathbf{m}	θ	α	$L = 100$	$L = 200$	$L = 300$	$L = \infty$
$(-1, 0, 0)$ $(+1, 0, 0)$	0.25	0	0.375018	0.375004	0.375002	0.375
$(-1, 0, 0)$ $(+1, 0, 0)$	0.25	0.25	0.374946	0.374986	0.374994	0.375
$(0, -1, 0)$ $(-1, -1, 0)$	0.25	0.25	0.375018	0.375005	0.375002	0.375
$(-1, 0, -1)$ $(-1, 0, +1)$	0.25	0	0.750368	0.750092	0.750041	0.75
$(-2, 0, 0)$ $(0, -2, 0)$	0.25	0	1.499419	1.499854	1.499935	1.5
$(0, -2, 0)$	0.25	0.25	1.499421	1.499854	1.499935	1.5

Table 1: A list of charge excitations labelled by the vector \mathbf{m} . We group in the same box excitations that have exactly the same excited eigenvalue. The scaling dimensions are estimated by solving numerically the BA equations for systems of increasing size L and making use of formula (5). Notice that the value of the scaling dimension does not depend on α . The last column shows the dimension predicted by formula (84).

\mathbf{m}, \mathbf{I}^+	θ	α	$L = 100$	$L = 200$	$L = 300$	$L = \infty$
$\mathbf{m} = (-1, 0, 0)$ $\mathbf{I}^+ = (1, 0, 0)$	0.25	0	1.373801	1.374700	1.374867	1.375
$\mathbf{m} = (-2, -2, -2)$ $\mathbf{I}^+ = (1, 0, 0)$	0.25	0	2.495597	2.498891	2.499506	2.5
$\mathbf{m} = (-2, -2, -2)$ $\mathbf{I}^+ = (1, 0, 0)$	0.25	0.25	2.4966007	2.499141	2.499617	2.5
$\mathbf{m} = (-2, -3, -2)$ $\mathbf{I}^+ = (0, 1, 0)$	0.25	0	2.871114	2.874015	2.874560	2.875
$\mathbf{m} = (-2, -3, -2)$ $\mathbf{I}^+ = (0, 1, 0)$	0.25	0.25	2.873027	2.874490	2.874771	2.875

Table 2: A list of excitations constructed combining the charged excitation labelled by the vector \mathbf{m} with the particle-hole excitation labeled by \mathbf{I}^+ . The scaling dimensions are estimated by solving numerically the BA equations for systems of increasing size L and making use of formula (5). In order to create the particle-hole excitation we insert a hole between the two particles that are located at the very end of the Fermi sea. Notice that for this class of excitations the scaling dimensions do not depend on the phase α . The last column shows the dimensions predicted by formula (84).

\mathbf{m}, \mathbf{e}	θ	α	L=100	L=200	L=300	$L = \infty$
$\mathbf{e} = (-1, 0, 0)$ $\mathbf{m} = (-1, 0, 0)$	0.25	0	1.373677	1.374668	1.374852	1.375
$\mathbf{e} = (-2, 0, 0)$ $\mathbf{m} = (-4, -4, -4)$	0.25	0	9.922879	9.980360	9.991231	10
$\mathbf{e} = (-1, 0, +1)$ $\mathbf{m} = (-2, -2, -2)$	0.25	0	2.829248	2.832285	2.832863	2.83
$\mathbf{e} = (+1, 0, +1)$ $\mathbf{m} = (-2, -2, -2)$	0.25	0	4.154368	4.163582	4.165295	4.16
$\mathbf{e} = (0, +1, 0)$ $\mathbf{m} = (-1, -2, -1)$	0.25	0	2.087041	2.084259	2.083745	2.083
$\mathbf{e} = (-1, +1, 0)$ $\mathbf{m} = (-2, -2, -2)$	0.25	0	2.875721	2.875168	2.875073	2.875
$\mathbf{e} = (+1, 0, 0)$ $\mathbf{m} = (-2, -2, -2)$	0.25	0.3	2.097194	2.099292	2.099684	2.1
$\mathbf{e} = (-1, 0, 0)$ $\mathbf{m} = (-2, -2, -2)$	0.25	0.3	2.893517	2.898372	2.899276	2.9

Table 3: A list of excitations constructed combining a variation in the number of “particles” labelled by \mathbf{m} , with transitions, from one side to other of the Fermi seas, labelled by \mathbf{e} . The scaling dimensions are estimated by solving numerically the BA equations for systems of increasing size L and making use of formula (5). Notice that for this set of excitations in which $\mathbf{e} \neq (0, 0, 0)$ the scaling dimensions exhibit a dependence on α . The last column shows the dimensions predicted by formula (84).

which confirms the results proposed independently in [3]. A formula of this type was derived for the first time in [23] for the conformal dimensions of models solvable by multicomponent Bethe ansatz. A rigorous proof of the fact that the scaling dimensions associated with the charge excitation and the umklapp process are essentially inverse of each other has been given in [22]. A similar expression for the conformal dimensions, in which \mathbf{C} is replaced by the Cartan matrix of sl_3 , has been found in [24] for a loop model on the hexagonal lattice.

9 Conclusions

We have derived a non-linear integral equation for the FPL² model on the critical part of the solvable line. As an application we have extracted exact expressions for the central charge and for the critical exponent associated with one black and one grey string propagating between two points on the lattice. We have also studied numerically the low-lying

excitations that can be constructed perturbing the Fermi seas in a more general manner (charge, umklapp and particle-hole excitations) and found that the scaling dimensions can be classified in a compact way through the Cartan matrix of sl_4 . The calculations have been done without having the knowledge of the underlying group structure discovered in [3] and constitute a confirmation of their results. It would be interesting to continue our study by considering strings excitations that can be generated selecting solutions of the BA equations in which some of the roots have an imaginary part different from zero.

A Appendix

A.1 The sums s_1 and s_2

Here we are going to show that the value of the central charge, which gives the dominant finite-size correction to the free energy density (42), is determined exclusively by the sum s_1 . The sum s_1 and s_2 has been defined as (43):

$$s_1 = \sum_{m=1}^{n_w} \varphi_1(w_m) \quad \varphi_1(x) = \log \left(\cos^2 \pi \theta + \sin^2 \pi \theta \coth^2 \frac{\pi \theta x}{2} \right) \quad (86)$$

$$s_2 = \sum_{m=1}^{n_w} \varphi_2(w_m) \quad \varphi_2(x) = \arctan(\tan(\pi \theta) \coth(\pi \theta x/2)). \quad (87)$$

The function $\varphi_1(x)$ has a singularity at the origin which, in deriving the integral expression for the free energy, will generate border terms. In particular it can be shown that:

$$\lim_{\eta \rightarrow 0^+} \frac{1}{\pi} \text{Im} \varphi_1(x + i\eta) \log \left[1 + \exp[iZ_{L,w}(x + i\eta)] \right] \Big|_{0^+}^{0^-} = 2(\log 2 + \log \cos(Z_{L,w}(0)/2)). \quad (88)$$

We checked numerically with fifteen digits of accuracy, that, for the ground state and the excited state under investigation, the term depending on s_2 , in the expression for the free energy (42), exactly cancels with the previous border term:

$$\log \cos(2\pi \alpha + s_2) - \log \cos(Z_{L,w}(0)/2) = 0 \quad (89)$$

so that the finite-size corrections to the free energy density are determined exclusively by the sum s_1 .

A.2 Lemma

Here, for completeness, we reproduce, following [31], the prove of formula (55).

Hypothesis:

Assume that $F(x)$ satisfies the non-linear integral equation (NLIE):

$$-i \log F(x) = \phi(x) + \int_{-\infty}^{+\infty} dy G(x-y) Q(y) \quad (90)$$

where the non-linear term $Q(x)$ is defined by:

$$Q(x) \equiv 2 \operatorname{Im} \log[1 + F(x + i\eta)] \quad (91)$$

assume also that the functions $\phi(x)$ and $G(x)$ are real and that $G(x)$ is symmetric, integrable and peaked around the origin.

Thesis:

Then the following identity holds:

$$\begin{aligned} \int_{-\infty}^{+\infty} dx \phi'(x) Q(x) &= -2 \operatorname{Re} \int_{\Gamma} \frac{du}{u} \log[1 + u] \\ &\quad - \frac{1}{2} [Q^2(+\infty) - Q^2(-\infty)] \int_{-\infty}^{+\infty} dx G(x) \end{aligned} \quad (92)$$

where Γ is a contour in the complex u -plane from $F(-\infty + i0^+)$ to $F(+\infty + i0^+)$ avoiding the logarithmic cut $(-\infty, -1]$.

Proof:

Deriving (90) and substituting the expression for $\phi'(x)$ into the lhs of (92) we get:

$$\begin{aligned} \int_{-\infty}^{+\infty} dx \phi'(x) Q(x) &= -2 \operatorname{Im} \int_{-\infty}^{+\infty} dx i \frac{F'(x)}{F(x)} \log[1 + F(x + i\eta)] \\ &\quad - \int_{-\infty}^{+\infty} dx \left[\int_{-\infty}^{+\infty} dy G'(x-y) Q(y) \right] Q(x) \end{aligned} \quad (93)$$

The first term on the rhs of (93) originates the dilogarithmic term in the rhs of (92). Let us examine in detail the double integral $I(a, b)$ where $0 < a < b$:

$$\begin{aligned} I(a, b) &= \int_{-a}^{+a} dx \left[\int_{-b}^{+b} dy G'(x-y) Q(y) \right] Q(x) \\ &= \int_{-a}^{+a} dx \left[\int_{-b}^{-a} dy G'(x-y) Q(y) + \int_{+a}^{+b} dy G'(x-y) Q(y) \right] Q(x) \end{aligned} \quad (94)$$

where we have used the fact that $G'(x)$ is an odd function. Integrating by parts:

$$\begin{aligned} I(a, b) &= \int_{-a}^{+a} dx \left[G(x+b) Q(-b) - G(x+a) Q(-a) + \int_{-b}^{-a} dy G(x-y) Q'(y) \right] Q(x) \\ &\quad + \int_{-a}^{+a} dx \left[G(x-a) Q(a) - G(x-b) Q(b) + \int_{+a}^{+b} dy G(x-y) Q'(y) \right] Q(x) \end{aligned} \quad (95)$$

In the limit $\lim_{a \rightarrow +\infty} [\lim_{b \rightarrow +\infty} I(a, b)]$ the integrals and the terms depending on b , inside the square brackets of (95), vanishes because $\lim_{x \rightarrow \pm\infty} G(x) = 0$. For the terms depending on a we can write:

$$\lim_{a \rightarrow +\infty} \int_{-a}^{+a} dx [\mp G(x \pm a) Q(\mp a) Q(x)] = \mp \frac{1}{2} Q^2(\mp\infty) \int_{-\infty}^{+\infty} dx G(x) \quad (96)$$

where we have used the fact that $G(x)$ is symmetric and peaked around the origin together with the assumption that $Q(x)$ tends to some asymptotic value in the limit $x \rightarrow \pm\infty$. The generalization to the multicomponent case [34] is straightforward.

References

- [1] D. Dei Cont, B. Nienhuis, *The packing of two species of polygons on the square lattice*. J. Phys. A **37** (2004) 3085. [cond-mat/0311244].
- [2] B. Nienhuis, *Tiles and colors*. J. Stat. Phys. **102** (2001) 981. [cond-mat/0005274].
- [3] J. L. Jacobsen and P. Zinn-Justin, *Algebraic Bethe Ansatz for the FPL² model*. [math-ph/0402008].
- [4] J. L. Jacobsen and J. Kondev, *Field theory of compact polymers on the square lattice*. Nucl. Phys. **B532** (1998) 635. [cond-mat/9804048].
- [5] J. L. Jacobsen, J. Vannimenus, *Finite average lengths in critical loop models*. J. Phys. A **32** (1999) 5455. [cond-mat/9903242].
- [6] J. L. Jacobsen, J. Kondev, *Conformal field theory of the Flory model of polymer melting*. [cond-mat/0209247].
- [7] J. L. Jacobsen, J. Kondev, *Continuous melting of compact polymers*. [cond-mat/0401504].
- [8] J. L. Jacobsen, J. Kondev, *Transition from the compact to the dense phase of two-dimensional polymers*. J. Stat. Phys. **96** (1999) 21. [cond-mat/9811085].
- [9] J. Kondev, J. L. Jacobsen, *Conformational entropy of compact polymers*. Phys. Rev. Lett. Vol **81**, No **14** (1998) 2922.
- [10] J. Kondev, *Liouville field theory of fluctuating loops*. Phys. Rev. Lett. Vol **78**, (1997) 4320. [cond-mat/9703113].
- [11] J. Kondev and C. L. Henley, *Four-coloring model on the square lattice: A critical ground state*. Phys. Rev **B** Vol **52**, (1995) 6628.

- [12] J. Kondev and C. L. Henley, *Kac-Moody symmetries of critical ground states*. Nucl. Phys. **B464** (1996) 540. [cond-mat/9511102].
- [13] J. Kondev, J. de Gier, B. Nienhuis, *Operator spectrum and exact exponents of the fully packed loop model*. J. Phys. A **29** (1996) 6489. [cond-mat/9603170].
- [14] N. Read in *Proceedings of the Kagomé Workshop*, ed. P. Chandra (NEC Laboratories, Princeton 1992).
- [15] E. H. Lieb, *Residual entropy of square ice*. Phys. Rev. Vol **162**, No **1** (1967) 162.
- [16] J. L. Cardy, *Conformal invariance and universality in finite-size scaling*. J. Phys. A **27** (1984) L385.
- [17] J. L. Cardy, *Operator content of two dimensional conformally invariant theories*. Nucl. Phys. **B270** (1986) 186.
- [18] H. W. J. Blöte, J. L. Cardy, M. P. Nightingale, *Conformal invariance, the central charge, and universal finite size amplitudes at criticality*. Phys. Rev. Lett. Vol **56** (1986) 742.
- [19] I. Affleck, *Universal term in the free energy at a critical point and the conformal anomaly*. Phys. Rev. Lett. Vol **56** (1986) 746.
- [20] V. S. Dotsenko, V. A. Fateev, *Conformal algebra and multipoint correlation functions in 2D statistical models*. Nucl. Phys. **B240** (1984) 312.
- [21] V. S. Dotsenko, J. L. Jacobsen, M. Picco, *Classification of conformal field theories based on coulomb gases. Application to loop models*. Nucl. Phys. **B618** (2001) 523. [hep-th/0105287].
- [22] N. M. Bogoliubov, A. G. Izergin and N. Yu. Reshetikhin *Finite-size effects and infrared asymptotics of the correlation functions in two dimensions*. J. Phys. A **20** (1987) 5361.
- [23] A. G. Izergin, V. E. Korepin and N. Yu. Reshetikhin *Conformal dimensions in Bethe ansatz solvable models*. J. Phys. A **22** (1989) 2651.
- [24] N. Yu. Reshetikhin, *A new exactly solvable case of an $O(n)$ -model on a hexagonal lattice*. J. Phys. A **24** (1991) 2387.
- [25] M. J. Martins, *Integrable mixed vertex models from braid monoid algebra*. In *Statistical physics on the eve of the 21-st century*, eds. M. T. Batchelor, L. T. Wille, Vol 14 of *Series on advances in Statistical Mechanics*, World Scientific, Singapore 1999. [solv-int/9903006].

- [26] P. A. Kalugin, *Low-lying excitations in the square-triangle random tiling model*. J. Phys. A **30** (1997) 7077.
- [27] M. T. Batchelor, J. Suzuki and C. M. Yung, *Exact results for hamiltonian walks from the solution of the fully packed loop model on the honeycomb lattice*. Phys. Rev. Lett. Vol **73**, No **20** (1994) 2646. [cond-mat/9408083].
- [28] M. T. Batchelor, H. W. J. Blöte, B. Nienhuis and C. M. Yung, *Critical behaviour of the fully packed loop model on the square lattice*. J. Phys. A **29** (1996) L399.
- [29] R. Raghavan, C. L. Henley, S. L. Arouh, *New two-color dimers models with critical ground state*. J. Stat. Phys. **86** (1997) 517. [cond-mat/9606220].
- [30] C. Destri, H. J. de Vega, *Unified approach to thermodynamic Bethe ansatz and finite size corrections for lattice models and field theories*. Nucl. Phys. **B438** (1995) 413. [hep-th/9407117].
- [31] C. Destri, H. J. de Vega, *Non linear integral equations and excited-states scaling functions in the sine-Gordon model*. Nucl. Phys. **B504** (1997) 621. [hep-th/9701107].
- [32] C. Destri, H. J. de Vega, *New thermodynamic Bethe ansatz equations without strings*. Phys. Rev. Lett. Vol **69**, No **16** (1992) 2313.
- [33] P. A. Pearce, A. Klümper, *Finite-Size corrections and scaling dimensions of solvable lattice models: An analytic method*. Phys. Rev. Lett. Vol **66**, No **8** (1991) 974.
- [34] P. Zinn-Justin, *Non-linear integral equations for complex affine Toda models associated to simply laced Lie algebras*. J. Phys. A **31** (1998) 6747. [hep-th/9712222].
- [35] P. Dorey, R. Tateo, *Excited states by analytic continuation of TBA equations*. Nucl. Phys. **B482** (1996) 639. [hep-th/9607167].
- [36] P. Dorey, R. Tateo, *Excited states in some simple perturbed conformal field theories*. Nucl. Phys. **B515** (1998) 575. [hep-th/9706140].
- [37] D. Fioravanti, A. Mariottini, E. Quattrini and F. Ravanini, *Excited states Destri-de Vega equation for sine-Gordon models*. Phys. Lett. **B390** (1997) 243. [hep-th/9608091].